Field Corrosion of 212 Main Rotor Blades – Analysis of EDX Results

Randy Lee

Bell Helicopter Textron

Assembly & Rotors, Design Quality & Engineering

May 2005

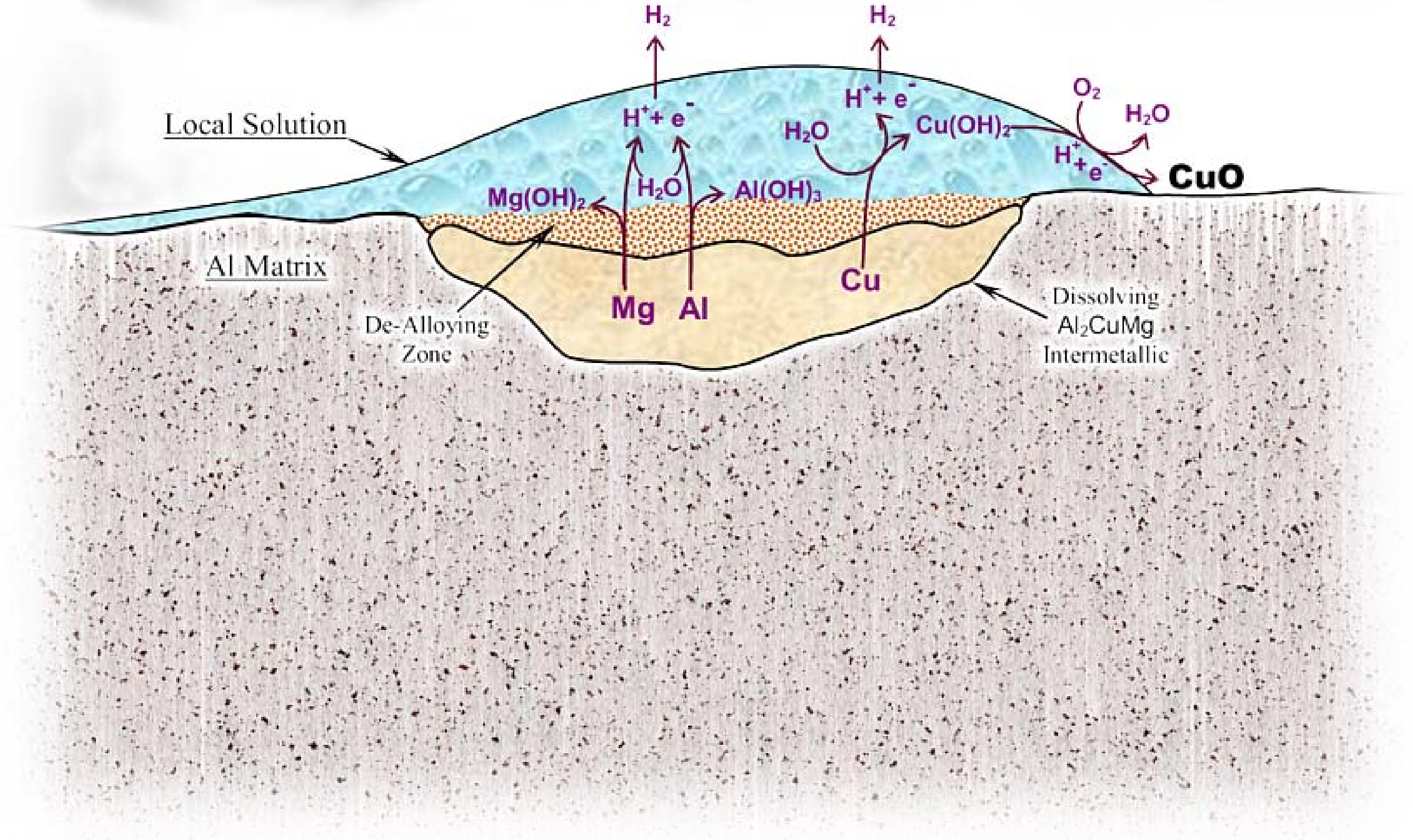

Introduction

Throughout industry, from electronic components to aircraft structures, whenever defects involving aluminum corrosion are evaluated, the most likely culprit has often been attributed to one of the halides. The most publicized mechanism postulates that, in the presence of ionized water, trace amounts of fluoride or chloride induce corrosive degradation when halide ions break down the native oxide (passivation) layer and permit attack of the exposed aluminum. Common chloride-based salt spray / salt fog tests are intended to simulate accelerated conditions, but these tests may not always provide accurate predictions (for example, see http://www.corrosion-doctors.org/TestingBasics/B117-Bogus-1.htm). While small quantities of chloride were detected in previous EDX tests, no halides were apparent in the data evaluated for this report. However, due to its notoriety, the chloride-induced mechanism provides a good example to facilitate the understanding of aluminum corrosion and more importantly, breach of the oxide layer (deoxidation), which must occur before degradation of the aluminum metal can begin. In addition to the halide ions (F^-, Cl^- and Br^-), other 'deoxidizing agents' have been reported to affect the stability (and degradative potential) of the oxide layer, more notably, the sulfate and hydroxide anions, SO_4^{2-} and OH^-.

The surface passivation layer is a very thin conversion coating (a few Angstroms thick) which is formed as a result of the initial corrosion reactions between surface aluminum atoms and atmospheric or local oxygen and moisture. This process produces aluminum oxide (alumina), Al_2O_3 throughout the conversion thickness but with higher levels of hydrated alumina, $Al_2O_3 \bullet H_2O$ and aluminum hydroxide $Al(OH)_3$ in the outermost region of the coating. Under nominal atmospheric conditions, the layer consists of natural oxidation/hydration products which grow from the outside surface *into* the aluminum body. The oxide conversion coating layer passivates the aluminum and inhibits additional oxidation/hydration (corrosion) of the bare metal. Since both oxygen and water are involved, oxidation and hydrolysis of bare aluminum occurs simultaneously, and the term 'hydrolytic oxidation' appropriately defines the corrosion process for bare aluminum. As an analogy, the oxide layer (alumina) is breached by reduction or deoxidation as part of the overall hydrolysis process, and an appropriate term for degradation of the oxide might be 'hydrolytic deoxidation'. The coating layer rapidly re-forms and repairs itself whenever disrupted, thus protecting the bare alumimum on a continual basis, indefinitely. By the action of an applied current, *anodizing* forms a much thicker (and controlled) version of the same oxide/hydroxide conversion product. In essence, the corrosion of 'ultra clean' aluminum in the presence of pure oxygen and water would be nothing more that an extension of these same growth processes. In all cases, exposed aluminum atoms are consumed (converted) to form the oxide and the hydroxide… but the degree, depth, and shape of the process into and throughout the aluminum body determines whether the effect becomes 'oxide protection' or 'corrosive degradation'. Generally, corrosive degradation would involve contaminants resulting in higher levels of aluminum hydroxide $Al(OH)_3$, which could be considered as the primary product of 'aluminum corrosion'. In actuality, corrosive degradation of aluminum is often a result of one or more possible corrosion mechanisms occurring simultaneously, such as intergranular galvanic interactions (between different metals), and pitting corrosion which penetrates even deeper into the aluminum body. Both conditions are highly probable mechanisms for the current problem at hand and will be considered in greater depth this study.

Besides magnesium, bare aluminum is one of the most anodic or active (corrosive) metals in common use. On the other hand, its rapidly forming surface layer makes it one of the most corrosion/oxidation-protective metals available. The problem deals with situations where the oxide layer is breached and hydrolytic oxidation agents are able to attack the exposed metal before the oxide has time re-form, which means that damage to the layer almost needs to occur while the aluminum is *in* the corrosive environment. In moist conditions and rough handling environments, the potential for initiation of corrosive degradation of aluminum bodies is quite high. Even in seemingly undisturbed storage conditions, if water is intermittently present or the aluminum is stacked/assembled in a high humidty environment, all that may be needed to initiate a degradative corrosion process are some trace amounts of a few naturally occuring ions, such as chloride, sulfide, sulfates, alkali, organic acids and salts, etc… Many of these are common surface contaminants and are found just about everywhere... on the floor, workshop surfaces, human skin debris and fluids, microbial particles, airborn dust particles, etc... However, it is the author's contention that, in addition to these commonly recognized contaminants and conditions, momentary localized pH changes are absolutely necessary to initiate degradation (breach) of the alumina layer. Merely the presenced of water, a basic deoxidizing anion and a few local contaminates are not enough, as implied from many studies. Consider the following scenario for halide-induced corrosion of alumina/aluminum as proposed for this current study. As the deoxidizing agents in this situation, chloride ions can easily diffuse through the porous hydroxide outer layer to gain access to the oxide Al_2O_3. If this regional point is also accompanied by a localized radical drop in pH, such as might be instigated by certain environmental contaminants or commonly occuring organic acid remnants, chloride ion can facilitate the hydrolysis of aluminum by reducing the oxide to form hydroxyl ions and the Lewis acid, aluminum chloride $AlCl_3$ …

$$Al_2O_3 + 6Cl^- + 3H_2O \xrightarrow[\text{Hydrolytic Deoxidation}]{H^+ + Na^+ \text{ or } Ca^{2+}} 2AlCl_3 + 6OH^- \tag{1}$$

Local alkali or alkaline cations may momentarily associate with hydroxyl ions which rapidly react with $AlCl_3$ to form the primary alumina degradation product, aluminum hydroxide $Al(OH)_3$ ...

$$AlCl_3 + 3OH^- \xrightarrow[\text{SN2-type Substitution}]{} Al(OH)_3 + 3Cl^- \tag{2}$$

Ultimately, oxide degradation will expose the bare aluminum metal to the local solution... unprotected. And just about any species in the local solution will readily react with exposed aluminum atoms. The mechanism depicted in Reactions (1) and (2) can be defined as the "hydroysis of native aluminum oxide via chloride deoxidation" which, as put forth here, can only take place at a point where there has also been an abrupt pH shift. Subsequent reactions directly involving the aluminum dissolution phase are covered later in the report.

For this quick study, the latest EDX test data generated for the 212 Corrosion Investigation Team was evaluated (provided during the March 30, 2005 Team Meeting). The test samples were taken from returned 212 blades (field returns) which were previously evaluated and then recently re-examined for this current study. Using the apparent EDX compositions given by the data, several scenarios are introduced which might be related to the type of corrosion effects exhibited in these test samples. A few common culprits associated with prolonged exposures to moist contamination are evaluated with emphasis on the ever important corrosive effects directly related to the various aluminum intermetallic phases present in aluminum alloys. Also, a number of detail parts (204/212 skins) were recently rejected prior to blade assembly operations due to apparent corrosion which had manifested itself on the aluminum surfaces primarily in the form of 'dirty' white precipitates. For these parts, the history of the raw material after receipt at Bell is uncertain. It is suspected that some of the aluminum sheet stock was exposed to moist, contaminated storage conditions after the initial machining operations. In all cases, the aluminum stock used by Bell for these details is supposed be typical aerospace grade 2024-T3 aluminum alloy whose primary alloying metal is copper. However, some of the EDX results acquired for the field test samples evaluated here indicate abnormally high levels of magnesium in the compositions. EDX compositional analysis also revealed the presence of a few possible contaminants that might be tied to previous corrosive degradation activities on the surface on the samples.

Experimental

History of Returned Blades and Sample Test Areas

Several 212 M/R blades have been returned over the last few years for reported corrosion problems concerning Blade Assemblies 212-015-501-115 and –119. A number of analysis were performed on the blades during that period by the M&M Lab, and at least three reports were issued. Those blades all contained several affected areas alleged to be corrosion, but repairs had already been attempted by field repair shops. For all practical purposes, the nature and extent of possible corrosion degradation in these affected areas is now indiscernible. Details regarding all of that activity has already been covered in previous reports and will not be considered here.

In this current analysis, a couple of those same blades were re-evaluated. This time however, several new areas (still covered with paint with no apparent defects) were subjected to plastic media blast to remove the coating and visually examined for possible corrosion defects which may not have advanced far enough to be noticeable on the external painted surface. The bulk of this activity was headed up by Chad Ford, Sr. M&P Engineer, M&M Lab. A couple of photos of the freshly exposed blade surfaces are given in Figure 1.

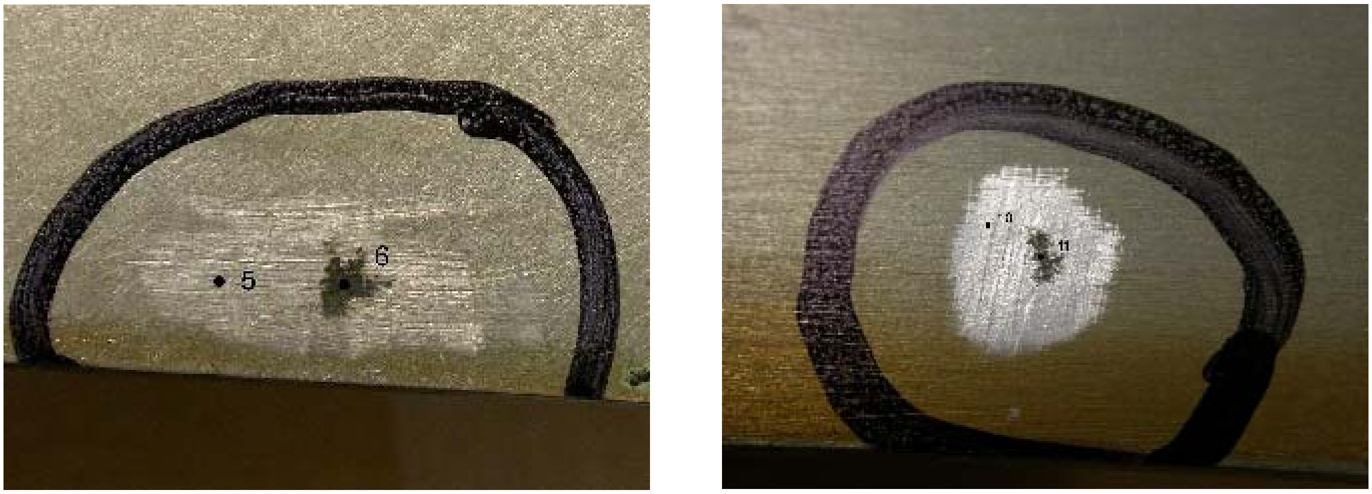

Figure 1 Areas of apparent corrosion exposed after coating removal via plastic media blast; Left image A-5361, Right image A-3434.

These photos indicate probable corrosion spots, black or dark gray in color, which had apparently been growing under the coating. Pitting is also characteristic in these areas as well as most of the other samples studied previously. It is also obvious that mechanical abrasion (sanding) has been performed on these areas at some point in their history, supposedly during repair/rework procedures. Concurrence with authorities in the Bell rework and repair departments confirmed that this work was not performed in-house either during normal manufacturing or field return rework operations. Therefore, it was concluded that these sanding patterns were most likely the work of outside field repair technicians serving the end customer. It is strongly suspected that field technicians noticed numerous spots such as these, suspected of being corrosion, after removing most or all of the coating from the blade during field shop processing for repair of the corrosion spots reported earlier. Furthermore, it is believed that these spots were much smaller at that time and have significantly progressed since then. In all likelihood, the technician(s) saw these ‘spots’ as small aberrations and swiped a sanding block across the areas a few times prior to re-painting. It is suspected that field repair personnel may have employed less-than-adequate techniques during their repair operations. Another perspective concerning the field repair operations will be noted later. However, it should be kept in mind that poor field workmanship (if factual) is not the cause of the initial corrosion conditions.

212-015-501-115 Blade Assy - Serial Number: A-3434 .. Final Date of Bell Assembly 1/4/97 .. Date of Shipment: 2/3/97 .. Date of Field Return Report: 2/3/04 .. Reported Use Hours: 1103 .. Purchase Customer: Agusta Un’Aziento, Italy .. End Use Customer: Italian Navy.

212-015-501-119 Blade Assy - Serial Number: A-5361 .. Final Date of Bell Assembly 1/13/03 .. Date of Shipment: 1/22/03 .. Date of Field Return Report: 2/3/04 .. Reported Use Hours: 146 .. Purchase Customer: Agusta Un’Aziento, Italy .. End Use Customer: Italian Navy.

Elemental analysis via SEM/EDX was performed by the M&M Lab on previous occasions for returned 212 blades exhibiting spots of apparent corrosion typically in the lower outboard region of the blades. For those test sets however, corresponding descriptions for each of the tested sample areas were not available. In this current series of EDX tests, several new sample areas were analyzed on the same blades (but in different areas) after coating removal via plastic media blast. For the current tests, brief descriptions were acquired for each of test areas. A table of the EDX results acquired by Chad Ford (M&M Lab) including the 'Test Area Description' is given in Table 1 below.

Table 1. EDX test results from the second series of analysis with Test Area Descriptions

Blade	Test Area Description	Test #	C	O	Mg	Al	Si	P	S	Ca	Ti	Cr	Mn	Fe
5361	Bare skin	1	41.59	9.53	1.43	44.87	0.89	0.00	0.00	0.00	0.36	0.22	0.13	0.06
	Same wiped with acetone	1A	22.93	0.00	11.44	62.93	0.61	0.00	0.27	0.00	0.32	0.28	0.15	0.08
	Abraded area	2	32.52	8.92	3.64	53.11	0.64	0.00	0.00	0.00	0.06	0.00	0.14	0.06
	Same wiped with acetone	2A	13.84	2.29	12.86	68.93	0.38	0.00	0.36	0.00	0.04	0.05	0.15	0.08
	Similar to 2 but different area	3	32.74	9.26	5.94	50.23	0.66	0.00	0.00	0.00	0.10	0.06	0.12	0.06
	Same wiped with acetone	3A	16.00	2.96	12.31	66.73	0.41	0.00	0.35	0.00	0.00	0.06	0.13	0.07
	Point analysis of 3	3 spot	25.18	13.84	6.83	49.94	0.83	0.00	1.22	0.00	1.12	0.00	0.16	0.00
	Apparent corrosion area on skin	4	48.95	17.15	4.55	26.05	1.36	0.00	0.10	0.22	0.57	0.44	0.06	0.05
	Point analysis of 4	4 spot	27.28	44.64	4.86	20.97	1.42	0.00	0.13	0.20	0.04	0.04	0.09	0.06
	Same wiped with acetone	4A spot	28.59	46.48	5.18	17.49	1.03	0.00	0.20	0.55	0.16	0.12	0.04	0.02
	Similar to 2 but more aggressive	5	12.81	0.00	11.55	73.25	0.75	0.00	0.18	0.00	0.13	0.00	0.16	0.07
	Same wiped with acetone	5A	11.70	3.42	12.75	70.31	0.27	0.00	0.27	0.05	0.00	0.00	0.15	0.06
	Point analysis of 5	5 spot	21.29	4.75	11.40	59.59	1.59	0.00	0.18	0.04	0.14	0.00	0.12	0.07
	Apparent corrosion area on skin	6	36.13	18.34	7.42	35.68	0.85	0.00	0.40	0.04	0.13	0.05	0.12	0.08
	Point analysis of 6	6 spot	39.57	39.08	5.43	12.91	1.43	0.00	0.54	0.03	0.27	0.08	0.11	0.05
	Same wiped with acetone	6A spot	29.16	46.32	5.20	16.81	0.97	0.00	0.55	0.03	0.06	0.03	0.10	0.04
	Apparent ding or dent in an abraded area	7	24.04	6.01	9.82	58.16	0.72	0.00	0.12	0.03	0.07	0.00	0.12	0.04
	Same wiped with acetone	7A	14.85	3.93	12.38	67.19	0.26	0.00	0.23	0.00	0.04	0.00	0.14	0.06
	Point analysis of 7	7 spot	12.78	0.68	12.70	71.81	0.54	0.00	0.18	0.00	0.05	0.04	0.19	0.07
3434	Bare skin	8	31.04	2.93	9.33	53.31	0.88	0.00	0.07	0.05	0.10	1.03	0.14	0.20
	Same wiped with acetone	8A	27.62	10.92	1.73	56.36	0.50	0.00	0.05	0.05	0.07	1.17	0.20	0.23
	Point analysis of 8	8 spot	16.38	5.91	10.80	63.62	0.39	0.00	0.00	0.11	0.00	1.39	0.15	0.27
	Bright spot (possible abrasion)	9	15.48	3.65	11.64	66.74	0.61	0.00	0.15	0.03	0.04	0.26	0.17	0.14
	Same wiped with acetone	9A	12.32	7.11	2.60	75.10	0.00	0.54	0.00	0.00	0.03	0.30	0.24	0.14
	Point analysis of 9	9 spot	16.92	1.78	11.41	67.16	0.59	0.00	0.11	0.00	0.10	0.27	0.26	0.33
	Abraded area	10	14.79	0.97	12.13	69.91	0.55	0.00	0.28	0.04	0.07	0.00	0.20	0.08
	Same wiped with acetone	10A	15.85	4.34	6.05	71.56	0.22	0.06	0.03	0.04	0.04	0.26	0.21	0.10
	Point analysis of 10	10 spot	13.04	1.29	12.38	71.16	0.49	0.00	0.31	0.00	0.04	0.05	0.21	0.11
	Apparent corrosion spot in 10	11	26.51	16.93	9.16	45.79	0.39	0.00	0.18	0.02	0.05	0.03	0.09	0.04
	Point analysis of 10	11 spot	35.66	39.53	4.44	18.38	1.00	0.00	0.32	0.19	0.05	0.04	0.07	0.03
	Same wiped with acetone	11A spot	7.78	57.53	3.63	29.04	0.64	0.45	0.27	0.15	0.00	0.03	0.10	0.00
	Bare skin, further inboard	12	38.76	9.03	7.02	43.28	0.39	0.00	0.00	0.03	0.03	0.47	0.08	0.14
	Same wiped with acetone	12A	23.66	5.96	8.34	59.66	0.42	0.09	0.00	0.05	0.00	0.55	0.10	0.16
	Point analysis of 12	12 spot	20.91	0.00	11.79	64.84	0.32	0.00	0.20	0.03	0.00	0.75	0.15	0.14
	Apparent corrosion area on skin	13	0.00	0.00	14.85	80.47	1.61	0.00	0.29	0.14	0.07	0.75	0.13	0.20
	Point analysis of 13	13 spot	68.08	0.00	6.06	19.54	3.32	0.00	0.25	0.22	0.41	0.09	0.03	0.09
	Same wiped with acetone	13A spot	0.00	13.48	11.34	72.72	0.14	0.11	0.11	0.08	0.04	0.61	0.09	0.08
	Anomaly, re-applied chemfilm?	14	38.83	0.00	9.15	46.21	1.10	0.00	0.08	0.22	0.15	2.38	0.09	0.92
	Same wiped with acetone	14A	12.35	4.19	3.95	23.83	0.32	0.24	0.00	53.31	0.02	0.71	0.06	0.20
	Point analysis of 14	14 spot	43.82	0.00	8.14	42.67	0.78	0.00	0.00	0.13	0.00	2.85	0.10	0.64
	Apparent corrosion on skin	15	9.77	53.94	5.81	26.75	0.97	0.38	0.64	0.12	0.12	0.05	0.05	0.03
	Apparent corrosion on skin	16	29.31	1.78	10.57	53.96	1.42	0.18	0.38	0.12	0.07	0.11	0.19	0.05
	Area EDX analysis/scans (100X) except 'Spot' tests, which are more focused (point) scans													

It might be kept in mind that compositional analysis via SEM/EDX is semi-quantitative. Sometimes, exact compositions can be surmized. Other times, the results may reveal very little, and sometimes, EDX results can be completely misleading. Compositions here are given in 'atomic percentages' which is roughly based on the 'number of atoms' in the sample. While EDX results can be provided (converted) in both atomic percent and weight percent, atomic fractions permit easier stoichiometric visualization at the onset. Weight fractions can later be converted to, if desired. All EDX tests performed here were done at electron bombardment energies of 25kV which means that some degree of penetration through the test layer into the Al substrate is inevitable. Thus, the results, while overwhelmingly characteriatic of the surface test material targeted, also represent the substrate composition to a degree.

There were questions regarding the nature and quantity of carbon indicated in most of these tests, in particular, whether the carbon was organic or inorganic in form. Subsequent to the initial EDX work, Chad Ford was kind enough to perform an acetone wipe on some of these sample areas and have the Organics Lab perform FTIR analysis of the washed sample surfaces prior to performing a post-wash EDX of the sample areas. FTIR results from those tests are given in Figure 2 along with some comments inserted by the author.

Figure 2 FTIR spectra of bare and corroded samples before and after acetone wipe.

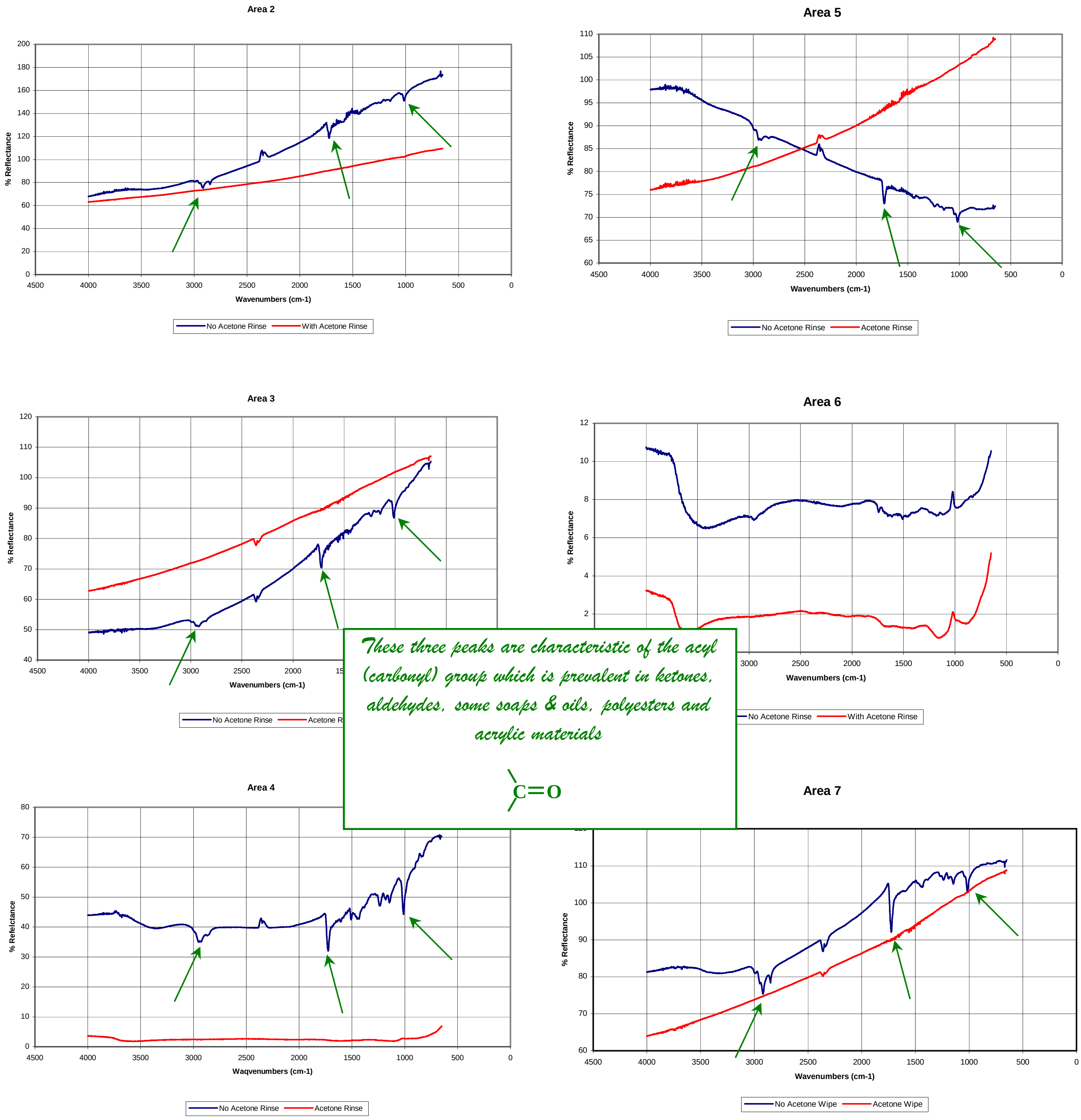

These three peaks are characteristic of the acyl (carbonyl) group which is prevalent in ketones, aldehydes, some soaps & oils, polyesters and acrylic materials

Analysis

If we rearrange Table 1 to compare only the EDX compositions for bare aluminum surfaces vs. corrosion areas side-by-side, much more is evident as shown in Table 2 below.

Table 2. EDX test results rearranged from Table 1

Blade	Test Area Description	Test #	C	O	Mg	Al	Si	P	S	Ca	Ti	Cr	Mn	Fe	Cu
5361	Bare skin	1	41.59	9.53	1.43	44.87	0.89	0.00	0.00	0.00	0.36	0.22	0.13	0.06	0.91
3434	Bare skin	8	31.04	2.93	9.33	53.31	0.88	0.00	0.07	0.05	0.10	1.03	0.14	0.20	0.93
3434	Point analysis of 8	8 spot	16.38	5.91	10.80	63.62	0.39	0.00	0.00	0.11	0.00	1.39	0.15	0.27	0.96
3434	Bare skin, further inboard	12	38.76	9.03	7.02	43.28	0.39	0.00	0.00	0.03	0.03	0.47	0.08	0.14	0.77
3434	Point analysis of 12	12 spot	20.91	0.00	11.79	64.84	0.32	0.00	0.20	0.03	0.00	0.75	0.15	0.14	0.87
5361	1 after acetone wipe	1A	22.93	0.00	11.44	62.93	0.61	0.00	0.27	0.00	0.32	0.28	0.15	0.08	0.98
3434	8 after acetone wipe	8A	27.62	10.92	1.73	56.36	0.50	0.00	0.05	0.05	0.07	1.17	0.20	0.23	1.11
3434	12 after acetone wipe	12A	23.66	5.96	8.34	59.66	0.42	0.09	0.00	0.05	0.00	0.55	0.10	0.16	0.96
5361	Apparent corrosion area on skin	4	48.95	17.15	4.55	26.05	1.36	0.00	0.10	0.22	0.57	0.44	0.06	0.05	0.49
5361	Point analysis of 4	4 spot	27.28	44.64	4.86	20.97	1.42	0.00	0.13	0.20	0.04	0.04	0.09	0.06	0.27
5361	Apparent corrosion area on skin	6	36.13	18.34	7.42	35.68	0.85	0.00	0.40	0.04	0.13	0.05	0.12	0.08	0.77
5361	Point analysis of 6	6 spot	39.57	39.08	5.43	12.91	1.43	0.00	0.54	0.03	0.27	0.08	0.11	0.05	0.51
3434	Apparent corrosion spot in 10	11	26.51	16.93	9.16	45.79	0.39	0.00	0.18	0.02	0.05	0.03	0.09	0.04	0.79
3434	Point analysis of 10	11 spot	35.66	39.53	4.44	18.38	1.00	0.00	0.32	0.19	0.05	0.04	0.07	0.03	0.29
3434	Apparent corrosion area on skin	13	0.00	0.00	14.85	80.47	1.61	0.00	0.29	0.14	0.07	0.75	0.13	0.20	1.50
3434	Point analysis of 13	13 spot	68.08	0.00	6.06	19.54	3.32	0.00	0.25	0.22	0.41	0.09	0.03	0.09	1.92
3434	Apparent corrosion on skin	15	9.77	53.94	5.81	26.75	0.97	0.38	0.64	0.12	0.12	0.05	0.05	0.03	0.79
3434	Apparent corrosion on skin	16	29.31	1.78	10.57	53.96	1.42	0.18	0.38	0.12	0.07	0.11	0.19	0.05	1.74
5361	4 after acetone wipe	4A spot	28.59	46.48	5.18	17.49	1.03	0.00	0.20	0.55	0.16	0.12	0.04	0.02	0.15
5361	6 after acetone wipe	6A spot	29.16	46.32	5.20	16.81	0.97	0.00	0.55	0.03	0.06	0.03	0.10	0.04	0.72
3434	10 after acetone wipe	11A spot	7.78	57.53	3.63	29.04	0.64	0.45	0.27	0.15	0.00	0.03	0.10	0.00	0.28
3434	13 after acetone wipe	13A spot	0.00	13.48	11.34	72.72	0.14	0.11	0.11	0.08	0.04	0.61	0.09	0.08	1.15
	Test 13 was omitted from the averages since oxides must be present in corrosion matter.														
	Spot' tests were not treated in the averages since areal scans are considered more representative of the general														
	composition of specific regions under test. Focused electron beam may even penetrate the substance of interest at 25kV through holes or low density points														

Scanning the numbers, column by column in the Bare Skin area and then those in the Corrosion area reveals some interesting differences. For instance, concentrations of both sulfur and calcium are notably higher in the corroded areas. However, the acetone wipe only removed a portion of the total carbon content. Lets us simply average these four groups, bare metal vs corroded metal along with their corresponding post-wash compositions as given in Table 3.

Table 3. Average EDX results for Bare vs. Corroded aluminum

	C	O	Mg	Al	Si	P	S	Ca	Ti	Cr	Mn	Fe	Cu
Bare	37.1%	7.2%	5.93%	47.2%	0.72%	0.00%	0.02%	0.03%	0.16%	0.57%	0.12%	0.13%	0.87%
Bare/Acetone	24.7%	5.63%	7.17%	59.7%	0.51%	0.03%	0.11%	0.03%	0.13%	0.67%	0.15%	0.16%	1.02%
Corroded	34.8%	25.4%	6.63%	30.5%	1.12%	0.03%	0.29%	0.12%	0.17%	0.11%	0.10%	0.05%	0.69%
Corroded/Acetone	21.8%	50.1%	4.67%	21.1%	0.88%	0.15%	0.34%	0.24%	0.07%	0.06%	0.08%	0.02%	0.38%

The unusually large fraction of carbon in all samples is not well understood, and its involvement in the corrosion process (if any) is uncertain. The unusually high increase in oxidation product after acetone wipe is also difficult to explain. The pre- and post- actetone-wipe results imply that most of the carbon was inorganic in form, implying the presence of carbonates and/or carbides. The author might have suggested a washing sequence consisting of hexane, toulene and THF for removal of general organics and polymers (spray & wash if possible – no wiping). However, acetone should have removed most of the free or loosely-bound organic entities. Acetone solubles should have included most nonionic organic molecules, monomers, oligomers, oils, waxes, most thermoplastics and some thermosets. Remnants might have included carbonates, carbides and possibly salts or dehydrated remnants of complex metals or organometallic compounds, if present. However, functional groups from these entities would have shown up in the post- IR spectra, as well as any possible associated acetone-oxidation products (acetone is not much of an oxidizing agent). Examination of Figure 1 indicates that the organic wash-off was high in carbonyl or acyl-bound carbon such as that found in ketones, aldehydes, acid derivatives and esters. There are two forms of plastic media acquired from Opti-Blast and used by Bell as called out in Material Bulletin 1687F, one being based on urea-formaldehyde and the other, methyl methacrylate (a polyester). The IR results (Figure 2) might be consistent with the ladder, and since nitrogen was not detected in the EDX scans, one could pretty much rule out urea-formaldhyde remnants, as well as any urethane-based coatings or amine-catalyzed epoxies for that matter.

As indicated in Table 3, changes in the carbon content before and after acetone wipe are about the same for both bare and corroded samples indicating that the level of inorganic carbon is about the same for both. Similarly, the amount or organic wash-off for both samples is also about the same. These observations might imply that the carbon entities (whether organic or inorganic) played no significant role in the corrosion process. For the moment, lets ignore the carbon component, as well as the effects of acetone wipe, and re-estimate Table 3 as given in Table 4 below.

Table 4. Average EDX results for Bare vs. Corroded aluminum – excluding the carbon fraction.

	O	**Mg**	**Al**	**Si**	**P**	**S**	**Ca**	**Ti**	**Cr**	**Mn**	**Fe**	**Cu**
Bare (-C)	11.4%	9.43%	75.0%	1.15%	0.00%	0.04%	0.04%	0.26%	0.91%	0.19%	0.21%	1.38%
Corroded (-C)	38.9%	10.2%	46.8%	1.72%	0.04%	0.45%	0.18%	0.26%	0.17%	0.16%	0.08%	1.06%

This method is an oversimplification and may not be error-free since it ignores possible nonlinear stochiometric effects between component fractions generated from the simple averages. With that in mind, let us attempt to evaluate Table 4 in efforts to identify possible mechanisms associated with the corrosion process. As mentioned earlier, *there are literally hundreds of possible reactions* that could have happened leading to the composition indicated in this analysis. We can only speculate and touch on a few selected scenarios in this paper. As redundant as it may sound, it should be kept in mind that we are comparing the surface composition of seemingly bare, non-degraded metal, to the apparent composition of some kind of suspect matter or aberration on top of the metal surface which is presumed to be corrosion product. Thus, knowing the composition of an unaffected bare spot vs. some surface crud elsewhere does not necessarily reveal or imply the corrosion sources, initial elements involved, any possible prevention mechanisms or whether the bare spot simply has not yet began to degrade.

First, lets make note of the apparent changes of bare vs. corroded compositions from Table 4. In the corroded area, the oxygen content is much higher, as one would expect. The aluminum fraction is significantly lower since much of it is presumedly combined with oxygen. Changes in silicon, phosphorus and manganese might be within the window of error for most SEM/EDX systems. The lower level of chromium in the corroded area indicates that the aluminum has lost much the oxidation protection imparted during factory processing. Surface level iron content might be lower in the corroded region as most of it has already oxidized as well. Copper can participate in intergranular and surface cathodic reactions with aluminum as well as forming intermetallic compounds. Effects of de-alloyed copper-rich intermetallics will be discussed later. The higher levels of sulfur and calcium may or may not provide an indication regarding the corrosion processes taking place. Possible corrosion mechanisms due to surface or environmental contaminants were introduced previously in reactions (1) and (2) and will be extended shortly.

First, the passivation layer is generated primarily by reaction of aluminum with oxygen, and by secondary interactions with water or humidity (which release hydrogen gas) during the corrosion (hydrolytic oxidation) process…

$$4Al + 3O_2 \xrightarrow[\text{Oxidation}]{} 2Al_2O_3$$

$$2Al + 3H_2O \xrightarrow[\text{Hydrolysis}]{} Al_2O_3 + 3H_2 \qquad \text{and} \qquad 2Al + 6H_2O \xrightarrow[\text{Hydrolysis}]{} 2Al(OH)_3 + 3H_2$$

The oxide (alumina) layer protects the aluminum from almost all environments. However, oxidation-protected aluminum bodies will readily dissolve in concentrated acids of hydrofluoric, hydrochloric and sulfuric as well as in concentrated bases such as NaOH or $Ca(OH)_2$. Conversely, nitric acid *does not* attack the oxide, but rather enhances the passivation effect (this is likely due to the relatively low electron affinity of nitrogen). The halide-induced hydrolysis/deoxidation/substitution scenario proposed in Reactions (1) and (2) provides a possible mechanism for degradation (breach) of the passive alumina layer via attack by chloride. While chloride was detected in previous EDX tests, there was none indicated in the current data. However, anions such as fluoride, hydroxide, sulfate and others will also form strong complexes with alumium ions. As mandated with the proposed chloride scheme, localized pH changes (below about pH 4 and above about 9) are required for degradation (etching) of the oxide to occur, regardless of which other ions may be present. This theory demands that a *highly localized momentary radical change in pH* is required to breach the oxide while simultaneously in the presence of Cl^-, OH^-, SO_4^{2-} (or possibly other anions). Bare aluminum is a fairly strong reducing agent... once exposed, almost anything will react with it, including water.

Note: Since magnesium is a significant component in the aluminum alloy under study, it should be noted that a similar set of reactions can be written for the natural oxidation/hydrolysis (passivation) of magnesium surfaces.

In heavy, localized concentrations, hydroxide ions OH^- will attack the Al_2O_3 structure, analogous to Reactions (1) and (2), but rather at locally *high* pH points and with formation of the aluminate ion…

$$Al_2O_3 + 2OH^- + 3H_2O \xrightarrow[\text{Hydrolytic Deoxidation}]{Ca^{2+} \text{ or } Mg^{2+}} 2Al(OH)_4^- \tag{3}$$

which can disproportionate to produce aluminum hydroxide and hydroxide ion...

$$Al(OH)_4^- \longrightarrow Al(OH)_3 + OH^- \tag{4}$$

Now the exact nature of the sulfur and calcium in the results is unknown, much less their predecessors (EDX only reveals the elements that are present and says nothing about their combined forms). The sulfur component might represent compounds of sulfate or sulfide with aluminum. Yellow aluminum sulfide will readily hydrolyze to the corresponding hydroxide while emitting hydrogen sulfide gas (stinky). Sulfides are also generated from sulfates during metabolic (anerobic) processing by certain bacteria. These sulfate-reducing bacteria will convert sulfates SO_4^{2-} into sulfides S^{2-}, and once in solution, sulfides readily hydrolyzed producing significant quantities of hydroxyl ions...

$$S^{2-} + H_2O \rightleftharpoons HS^- + OH^-$$

which can proceed to attack the oxide layer according to reactions (3) and (4).

If successors to soluble aluminum sulfate are indicated by the analysis, local surface contaminates containing the sulfate ion SO_4^{2-} could have been present at one time accompanied by a rapid local decrease in pH and following a mechanism similar to that proposed in Reactions (1) and (2)…

$$Al_2O_3 + 3SO_4^{2-} + 3H_2O \xrightarrow[\text{Hydrolytic Deoxidation}]{H^+ + Ca^{2+} \text{ or } Mg^{2+}} Al_2(SO_4)_3 + 6OH^- \tag{5}$$

$$Al_2(SO_4)_3 + 6OH^- \xrightarrow[\text{SN2-type Substitution}]{} Al(OH)_3 + 3SO_4^{2-} \tag{6}$$

Sulfates are abundant in almost all natural and tap waters, including rain. Contamination sources might also include metal finishing lines, organic salts, soaps & shampoos, gypsum (calcium sulfate), polluted air, acid rain, etc... The likelihood of SO_4^{2-} as a surface contaminant is greatly increased by the presence of alloyed copper and copper-rich phases on the surface of the exposed aluminum (this topic will be dealt with later in the report).

Consider the presence of calcium sulfate $CaSO_4$ or the oxide CaO (lime). $CaSO_4$ is the primary component in gypsum; it is also present in chalk, clays, talc, cement powders, body puddies, and is quite prevalent in hard (tap) water. Hydroxide ions will convert $CaSO_4$ to the corresponding hydroxide $Ca(OH)_2$, a very strong base, as will the reaction of CaO with water, both of which can then follow Reactions (5) and (6) or (3) and (4) to breach the oxide...

$$CaSO_4 + 2OH^- \longrightarrow Ca(OH)_2 + SO_4^{2-} \qquad \text{and} \qquad CaO + H_2O \longrightarrow Ca(OH)_2$$

Once in solution, aluminum atoms tend to form coordinated complexes rather quickly (usually hexavalent) often with many organic compounds, particularly acids such as formic, citric and glycolic, as well as with water itself...

$$Al^{3+} + 6H_2O \longrightarrow Al(H_2O)_6^{3+}$$

The complexed form will remain in solution longer and has enhanced activity in many reduction-oxidation (redox) reactions. The simplified notation Al^{3+} is generally used to represent the complexed (solvated) form. Since organic ligands could not be confirmed from the IR analysis, they likely did not play a role in the corrosion process. However, it might be noted that the high vacuum in the SEM/EDX chamber probably dehydrated all the samples anyway.

Note: While aqueous solutions of aluminum may tend to accommodate 6 coordinating groups, solid solutions or crystals of aluminum will typically exhibit a coordination number of 12 in accordance with aluminum's (face centered) cubic close-packed structure.

Bare aluminum is amphoteric, and its reactions with water, acids and bases again, involve hydrolytic oxidation. All reactions produce hydrogen gas and will occur spontaneously. While reaction with water precipitates white aluminum hydroxide (and/or alumina), reactions with acid and base put the aluminum into solution as its trivalent ion (hexahydrate complex) and aluminate ion respectively, and both can fall out of solution (precipitate) depending on the particular cations and anions that are locally available as well as the local pH...

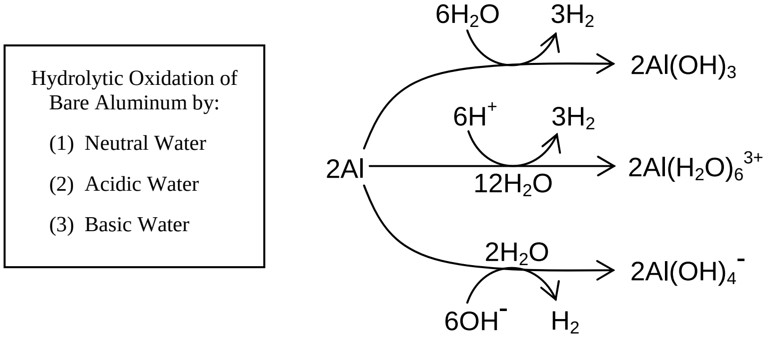

Note: Magnesium will also interact with water, acids and bases in a very similar fashion, except more aggresively.

In an aqueous solutions containing mixtures of ions such as Al^{3+}, SO_4^{2+}, Ca^{2+}, along with localized variable concentrations of acids and bases H^+, OH^-, a multitude of possible reactions could occur, many perhaps producing some very complicated mineral-type products such as the two illustrative examples given here...

$$\begin{gathered} a\,Al^{3+} + b\,Ca^{2+} + c\,SO_4^{2-} + d\,H_2O \longrightarrow Ca_wAl_x(SO_4)_y(OH)_z \cdot e\,H_2O + f\,H^+ \\ a\,Al^{3+} + b\,Ca^{2+} + c\,H_2O \longrightarrow Ca_wAl_xH_yO_z + d\,H^+ \end{gathered} \tag{7}$$

These compounds are not unlike some of those found in geological formations and common Portland cement.

Application of chromate films and rinses during Bell processing impart exceptional oxidation/corrosion protection to aluminum detail parts during the assembly phase and are intended to last throughout the field-use life cycle. Acidic chromate conversion coating solutions such as Alodine and ChemFilm are based on dichromate ($Cr_2O_7^{2-}$) which is a strong oxidizer, and also include a fluoride activator F^- (an extremely strong etchant for Al and Si oxides), as well as an accelerator, ferricyanide (an iron cyanide compound), which is needed to facilitate effective coversion rates on aluminum substrates. Non-activated chromate rinses are closer to neutral pH and do not generally attack the oxide, but rather, leave behind residues of chromate which can provide supplemental corrosion protection in addition to that imparted from conversion coating processes. During a chromate conversion process, both the passive aluminum oxide and bare aluminum participate in production of the final complex mixture which reduces Cr(VI) to Cr(III) in the initial layer of conversion product as illustrated in the following likely scenario...

(a) $$Al_2O_3 + 3H_2O \xrightarrow{HF} 2Al(OH)_3$$ Dissolution/Hydrolysis of the Oxide

(b) $$2Al \xrightarrow{3H_2O \curvearrowright 6H^+ + 6e^-} Al_2O_3$$ Oxidation/Hydrolysis of Bare Aluminum

(c) $$\underset{\text{Dichromate Ion}}{Cr_2O_7^{2-}} \xrightarrow{8H^+ + 6e^- \curvearrowright 4H_2O} \underset{\text{Chrome(III) Oxide}}{Cr_2O_3}$$ Reduction of Chromate Cr(VI) to Cr(III)

(d) $$2Al + \underset{\text{Cr(VI)}}{Cr_2O_7^{2-}} \xrightarrow{2H^+ \curvearrowright H_2O} Al_2O_3 + \underset{\text{Cr(III)}}{Cr_2O_3}$$ Overall Redox Reaction (Less Oxide Dissolution)

Most chromate rinses are prepared directly from dark red chromium trioxide crystals while conversion solutions are generally formulated using a dichromate salt (for example, potassium dichromate crystals are orange). Dichromate is the dominant species in acidic solutions and each anion will coordinate with four water molecules producing an orange solution. On the other hand, chromate (or 'mono-chromate') anions are stable in neutral and basic media and each will complex with six water molecules giving a yellow solution. Acidic systems formulated from the trioxide will convert into the dichromate (via dimerization via condensation), while neutral/basic solutions prepared from a dichromate salt will convert into the (mono) chromate. Both forms produce the same chromium oxidation state in solution, namely Cr(VI). Also, upon reduction, both forms give the green-yellow trivalent chromium Cr(III) oxide deposit. These properties are illustrated in the following reactions (complexed water molecules not shown)...

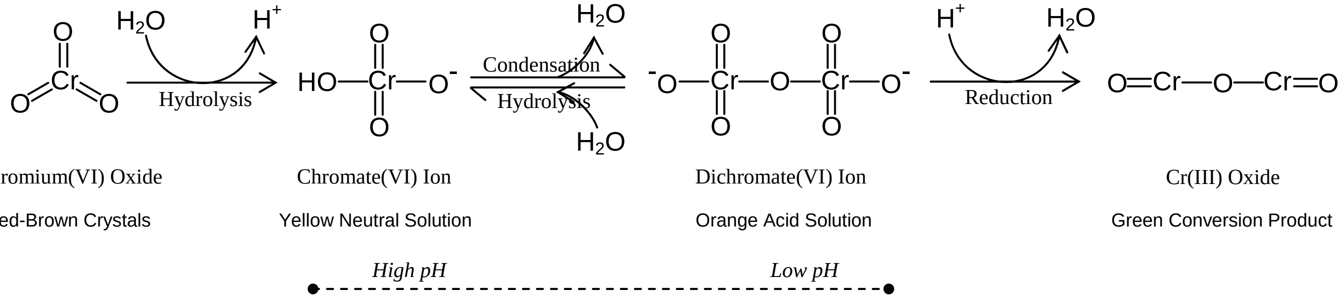

Now the reduction of chromate or dichromate from Cr (VI) to Cr (III) should produce not only the oxide (as in the reaction above and Reaction c), but also a significant proportion of the corresponding green hydroxide...

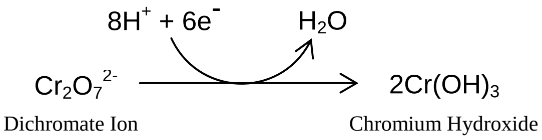

$$Cr_2O_7^{2-} \xrightarrow[\quad]{8H^+ + 6e^- \quad H_2O} 2Cr(OH)_3$$

Likewise, it is expected that oxidation/hydrolysis of bare aluminum generates not only the oxide (as shown in reaction b above), but the hydroxide as well. Ordinarily, these oxides and hydroxides would readily dissolve in the acidic halide solutions of Alodine and ChemFilm, except that they be protected by complexation or networking during the conversion process. Thus, it is believed that the initial conversion deposition layer is comprized of a complex, insoluble mixture containing: (1) aluminum oxide Al_2O_3, (2) aluminum hydroxide $Al(OH)_3$, (3) chromium(III) oxide Cr_2O_3, and (4) chromium(III) hydroxide $Cr(OH)_3$. These Cr(III) compounds are capable of providing sacrificial protection to the aluminum substrate by themselves oxidizing to the Cr(VI) state. However, if this were the only form of protection afforded by the coating, its benefits would be limited. It is believed therefore, that after formation of the initial Cr(III)-rich layer/deposit, hydroxyl groups in this layer attract and combine (via condensation-type reactions) with additional Cr(VI) dichromate ions readily available in the process solution. Furthermore, it is proposed that a limited degree of acid-catalyzed condensation-type polymerization occurs in both layers. This results in a dually-protective, brownish or gold-tinted system containing a Cr(VI) oxidation barrier on top of (and binded to) a Cr(III) sacrificial underlayer to form the Cr(III)-Cr(VI) and Cr(III)-Cr(VI)-Al(III) complex configuration as simplified in the following scenario...

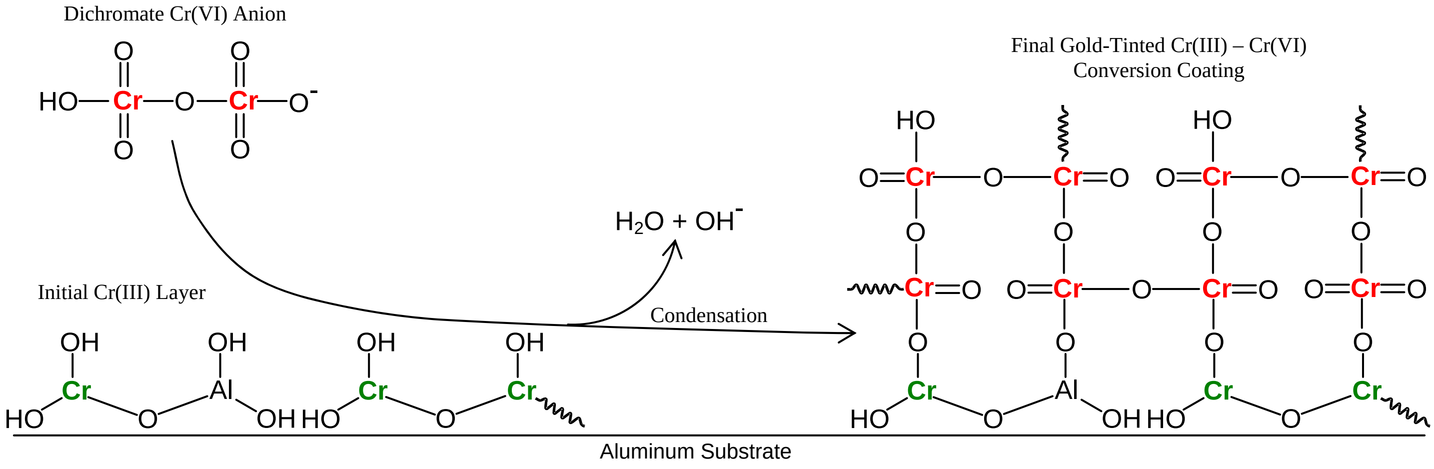

Since these complexes are strongly bound to the aluminum surface (and to themselves), the actions required to remove or deplete them (other than heat or strong acids) are somewhat limited. However, EDX results for the corroded samples reveal notably lower concentrations of chromate in these repaired areas. As inferred in the Experimental section, it is suspected that field repair personnel may have employed less than adequate techniques during the repair process (which included ChemFilm application). Of course, this does not justify the existence of corrosion seeds in the repaired areas to begin with. There is also a possibility that low initial concentrations of bound chromate could have been related to some specific aspect of the finishing process, or possibly some event that occurred in a subsequent operation, or... the presence of de-alloyed *intermetallic compounds* which could be due to inadequate heat treatment by the vendor or improper storage/aging after receipt at Bell, or both.

Chromate conversion rates differ significantly between the aluminum matrix and the various intermetallic phases which are known to exist. This means that the coating layer is heterogeneous across the aluminum surface. There are many possible intermetallic compounds characteristic to 2024 alloys which arise due to reactions between de-alloyed Al, Cu, Mg, Mn, Si and Fe. Intermetallic regions vary in size and may be located within the body of the alloy or on the surface. Depending on the particular stoichiometries formed, intermetallic compounds may emphasize the properties of one elemental constituent over another. There is a strong suspicion that the iron cyanide accelerator in Alodine and ChemFilm (usually in the form potassium ferricyanide, $K_3Fe(CN)_6$) inhibits growth of the conversion coating onto Cu-rich intermetallic surfaces. The coating thickness on Cu-rich intermetallic phases can be as little as one-tenth that on Al matrix surfaces. To say the least, the presence of intermetallic phases complicates the formation of conversion coatings on aluminum alloy surfaces. However, since the conversion rate of chromate with pure Al is slow to begin with, an accelerator is required in the solution formulation to enhance the conversion process on Al-rich substrates. The chelated nature of iron in this particular complex supplements the reduction of chrome from Cr(VI) to Cr(III) via oxidation of iron from Fe(II) to Fe(III). On pure Al phases, the conversion rate is increased when Fe(III) in ferricyanide is reduced to Fe(II) by way of reaction (b) above, followed by oxidation back to Fe(III) to facilitate the reduction of Cr(VI) to Cr(III) per reaction (c).

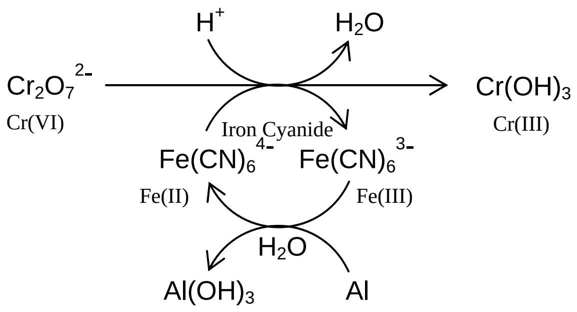

Augmented version of Reaction (c)

Some studies have reported the incorporation of cyanide remnants into the deposit. The 212 Corrosion Investigation Team had once considered the possibility that remnants from the chromate conversion solution might be a primary contributor to the suspected corrosion problem. Solution remnants (salts from unreacted components) could be present if workers used inadequate rinsing procedures after application of Alodine or ChemFilm. Without a doubt, effective rinsing and removal of ChemFilm/Alodine remnants is mandatory since unreacted salts containing flouride or cyanide can induce corrosion later on. However, EDX results do not support this theory since there were no detectible traces of fluorine, sodium or nitrogen on sample test areas.

In addition to varying reactivities toward chromate conversion, de-alloyed intermetallics play a critical role in the corrosion of Al alloys because they can act as anodes or cathodes forming galvanic couples within the material. In effort to better understand the potential corrosive and intermetallic effects associated with the constituents in our Al 2024 samples, a more focused look at just the metallic components from the EDX test data is in order. Table 4 can be re-estimated to incompass only the metallic components. But first, the industry standard ASM Aerospace Spec provides an average weight composition for the various aluminum alloys and has been used to estimate approximate atomic fractions for 2024 alloy by applying the method given in Table 5 below.

Table 5. Method and results for estimating average ASM 2024 aluminum atomic fractions.

	Al	**Cu**	**Mg**	**Mn**	**Si**	**Fe**	**Zn**	**Ti**	**Cr**
Atomic Weight	27.0	63.6	24.3	54.9	28.1	55.8	65.4	47.9	52.0
2024 ASM %Wt.	92.7	4.35	1.50	0.60	0.30	0.25	0.15	0.10	0.05
mol / 100g sample	3.433	0.068	0.062	0.011	0.011	0.004	0.002	0.002	0.001
Atomic Percentage	95.5%	1.90%	1.72%	0.30%	0.30%	0.12%	0.06%	0.06%	0.03%

Using Table 5 and the transformed data from Table 4 (excluding Ca), a side-by-side comparison is given in Table 6 below for the average metallic fractions in Bare and Corroded areas, along with published ASM averages for 2024 alloy (in atomic percentages). As inferred earlier, this method of eliminating and re-estimating selected components is less than ideal and is only used here as a simple, rough approximation.

Table 6. Average EDX results for Bare, Corroded Samples and ASM 2024 averages.

	Mg	**Al**	**Si**	**Ti**	**Cr**	**Mn**	**Fe**	**Cu**	**Zn**
Bare (M only)	10.6%	84.7%	1.29%	0.29%	1.03%	0.21%	0.24%	1.56%	0.00%
Corroded (M only)	16.8%	77.5%	2.85%	0.43%	0.29%	0.26%	0.13%	1.76%	0.00%
ASM 2024 -T3, -T4	1.72%	95.5%	0.30%	0.06%	0.03%	0.30%	0.12%	1.90%	0.06%

According to this version of the data, the Al sheet stock used for these blades appears to be extraordinarily high in Mg content (in lieu of Al), and notably high in Si. The abundant Mg levels here would almost lead one to think this alloy was from the 5XXX series rather than 2XXX. At room temperature, alloyed concentrations of Si greater than about 1% will precipitate out and oxidize. Alternatively, high surface levels of Si could indicate possible SiO_2 abrasive remnants (or perhaps more evidence of an alloy formulation gone awry). Magnesium is the only ‘structural’ metal in this composition that is more active (anodic) than aluminum and thus, it will oxidize first, forming a poorly protecting oxide/hydroxide product, in the form of MgO and $Mg(OH)_2$. In fact, de-alloyed Mg should sacrificially protect the Al matrix, tending to keep it in reduce form according to the simple redox reactions...

$$3Mg \xrightarrow{\qquad} 3Mg^{2+} + 6e^- \qquad \text{and} \qquad 2Al^{3+} + 6e^- \xrightarrow{\qquad} 2Al$$

$$\text{EMF} = 2.38\text{ V} \qquad\qquad \text{EMF} = -1.66\text{ V}$$

There are many tables containing the Standard Electrode Reduction Potentials (or EMF values) relative to hydrogen. However, some of these tables can contain hundreds of cathode/anode reactions, many or most of which are not relevant to the conditions under study here. So Table 7 has been constructed using some of the particular redox reactions which may be more relevant to our particular system (data compiled from the Internet).

Table 7. Simplified list of standard EMF Potentials (Activity Series) for reactions of current interest.

Oxidized Form		*Reduced Form*	*Volts*	
$Ca^{2+} + 2e^-$	$\rightleftharpoons$	Ca	-2.76	↑ Reverse reaction more likely ↓ Forward reaction more likely
$Mg^{2+} + 2e^-$	$\rightleftharpoons$	Mg	-2.38	
$Al^{3+} + 3e^-$	$\rightleftharpoons$	Al	-1.66	
$Mn^{2+} + 2e^-$	$\rightleftharpoons$	Mn	-1.19	
$2H_2O + 2e-$	$\rightleftharpoons$	$H_2 + 2OH^-$	-0.83	
$Cr^{3+} + 3e^-$	$\rightleftharpoons$	Cr	-0.74	
$Fe^{2+} + 2e^-$	$\rightleftharpoons$	Fe	-0.41	
$Fe^{3+} + 3e^-$	$\rightleftharpoons$	Fe	-0.04	
$2H^+ + 2e^-$	$\rightleftharpoons$	H_2	0.00	
$Cu^{2+} + e^-$	$\rightleftharpoons$	Cu^+	0.16	
$S + 2H^+ + 2e^-$	$\rightleftharpoons$	H_2S	0.17	
$Cu^{2+} + 2e^-$	$\rightleftharpoons$	Cu	0.34	
$Cu^+ + e^-$	$\rightleftharpoons$	Cu	0.52	
$Fe^{3+} + e^-$	$\rightleftharpoons$	Fe^{2+}	0.77	
$O_2 + 4H^+ + 4e^-$	$\rightleftharpoons$	$2H_2O$	1.23	
$Cr_2O_7^{2-} + 14H^+ + 6e^-$	$\rightleftharpoons$	$2Cr^{3+} + 7H_2O$	1.33	

As can be seen from Table 7, all other metals in our composition (Table 6) except Mg (and Ca) are cathodic to Al, which means that Al tends to protect them instead of the other way around. Galvanic properties between the various intermetallic compounds in 2024 alloy is not as straightforward as with these more common reactions.

Some of the more notable 2024 intermetallic compositions include Al_2Cu, Al_3Fe, AlCuMg, Al_2CuMg, Mg_2Si and Al_3Mg_2, as well as the eutectic $Al_{24}Cu_2Mg_7$. De-alloyed Cu-rich phases are quite cathodic to Al and can produce significant corrosion potentials leading to the formation of localized galvanic cells from which subsequent hydrolytic oxidization (corrosion) of Al will occur in moist conditions. In 2024 alloys, Cu-rich intermetallic phases, particles, grains or inclusions can provide favorable nucleation sites for initiation of pitting and intergranular corrosion. A couple of the more prevalent 2024 intermetallics are Al_2Cu and Al_3Fe, which are known to act cathodically towards Al causing corrosion along with the production of white Al oxides and hydroxides. Also, natural sulfation (via atmospheric SO_2) of Cu-rich areas lends credence to a theory supporting Reactions (5) and (6) as a likely method of oxide breach.

Pitting corrosion is a big problem with many of the self-passivating metals, especially Al alloys. Pitting is believed to be one of the major forms of corrosive degradation observed in the test samples evaluated for this study, as well as several corroded detail parts found in the early blade assembly process. Pit growth is highly dependent on the nature of contaminants and ions in the local environment (or local solution), and the local pH, as well as any galvanic effects associated with neighboring intermetallic granules or phases. Pit growth proceeds *into* the substrate at the point of oxide breach forming a 'crater' while the large area just outside the pit/crater is cathodically protected by reduction of local oxygen. At the same time, the breached point exposes bare Al to the local solution of contaminates which begin to dissolve the Al matrix. Electrons generated by oxidation and dissolution of Al in the pit migrate to the cathodic edges where they facilitate the reduction of oxygen with the release of hydrogen gas. Thus, the growing pit becomes the anode, increasing in H^+ concentration (decreasing in pH) and dissolved Al^{3+} content, while the surrounding pit edges (periphery) become the cathode, increasing in OH^- concentration (increasing in pH) and generating white aluminum hydroxide $Al(OH)_3$ as described in the following scheme...

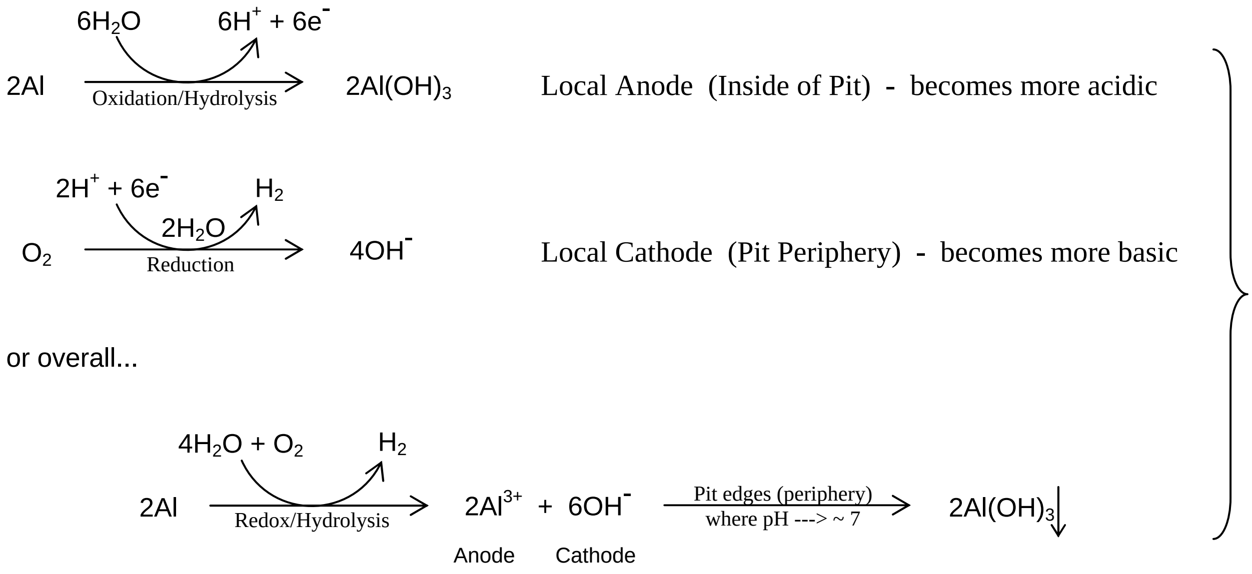

$$2Al \xrightarrow[\text{Oxidation/Hydrolysis}]{6H_2O \;\curvearrowright\; 6H^+ + 6e^-} 2Al(OH)_3 \quad \text{Local Anode (Inside of Pit) - becomes more acidic}$$

$$O_2 \xrightarrow[\text{Reduction}]{2H^+ + 6e^- \;\curvearrowright\; H_2,\ 2H_2O} 4OH^- \quad \text{Local Cathode (Pit Periphery) - becomes more basic}$$

or overall...

$$\underset{}{2Al} \xrightarrow[\text{Redox/Hydrolysis}]{4H_2O + O_2 \;\curvearrowright\; H_2} \underset{\text{Anode}}{2Al^{3+}} + \underset{\text{Cathode}}{6OH^-} \xrightarrow[\text{where pH ---> ~ 7}]{\text{Pit edges (periphery)}} 2Al(OH)_3\downarrow \qquad (8)$$

Pit growth is strengthened tremendously when the oxide breach occurs in the vicinity of a Cu-rich intermetallic phase which can induce galvanic coupling. Thus, the anodic reaction is driven strongly by the local pH and intermetallic-induced galvanic potential while the cathodic reaction is almost entirely diffusion controlled. Initiation of pitting corrosion involves breaching/etching or loss of the oxide by (1) mechanical damage, or (2) chemical attack (as covered in Reactions 1 & 2, 3 & 4, and 5 & 6). Using Reactions (8), such a condition is illustrated in Figure 3.

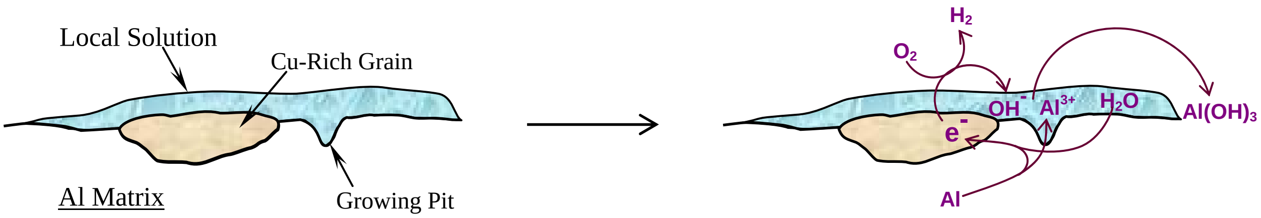

Figure 3. Diagram of galvanic couple between Cu-rich grain and pitted Al with associated reactions.

Many aluminum corrosion problems throughout various industries have reported the production of white precipitates. Without a doubt, this is due to formation of the oxide and hydroxide of Al, as well as the same for Mg if present in the alloy - all clear-to-white crystalline particles. White precipitates have also been observed on detail parts undergoing Bell process/assembly operations suspected of being defective due to corrosion. However, as the two images in the Experimental section indicate (Figure 1), the defective areas appear gray-to-black and there is no visible evidence of white precipitates. For reference, enlargements of those photos are given in Figure 4.

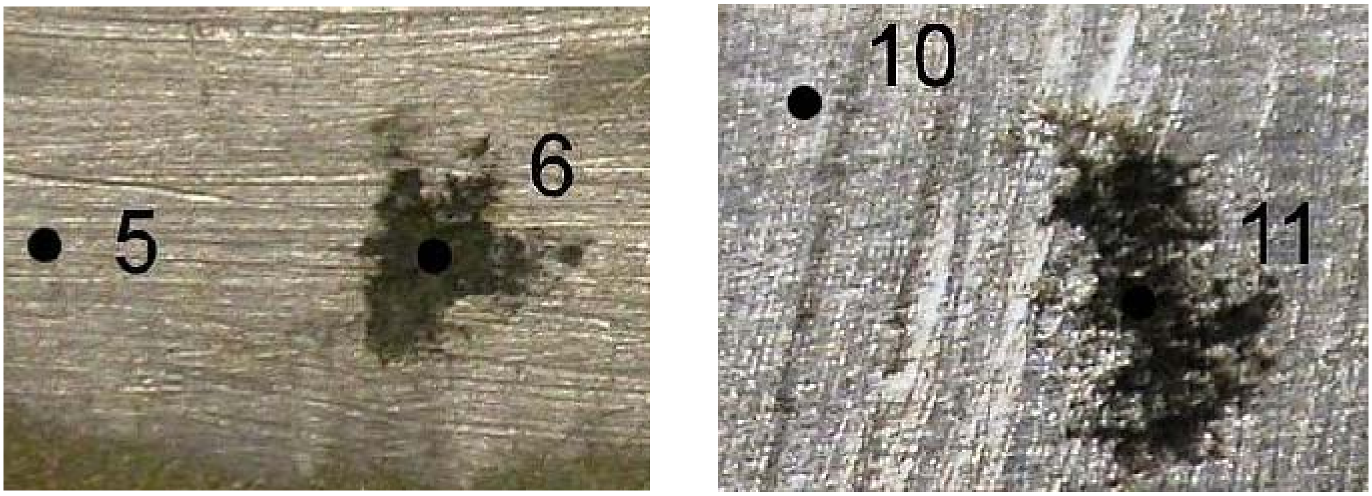

Figure 4. Magified views of corroded sample areas after media blast, as taken from Figure 1.

While it is likely that remnants of white corrosion products could have been removed and blown away during media blast, these obvious darker corrosion effects have not been accounted for. Traditional theories dealing with aluminum corrosion almost always include formation of hydroxide and oxide precipitates as noted above. Contrary to more popular mechanisms which tend to follow classical thermodynamics (such as the Nernst equation), dissolution of cathodic Cu-rich particles followed by their oxidation to black copper oxide is believed to be quite possible. On the other hand, in situations where the intermetallic phase is rich in Mg, the mechanism dipicted in Figure 3 is essentially reversed and no degradation of the Al will occur. Rather, the Mg-rich granule will itself begin to dissolve since it is anodic to the surrounding Al matrix. Some of the intermetallics which are likely to be more active than (anodic to) Al, would include compounds such as Al_2CuMg, Al_3Mg_2 and Mg_2Si, all of which could raise the local potential high enough to induce corrosive reactions. Many of these Al-rich/Mg-rich anodic intermetallics also contain Cu to varying degrees which will dissolve in the local solution and oxidize, deposit or precipitate somewhere in the vicinity.

As an analog to the condition given in Reactions (8) and Figure 3, consider the following proposed mechanism. An anodic intermetallic particle, say of Al_2CuMg, is embedded in the Al surface, and the local area is again exposed to a contaminated, moist environment (as in Fig 3). Then the following simplified reaction scenario might occur in the local galvanic macro-sphere. Within the immediate vicinity of the dissolving intermetallic phase, both Mg and Al undergo oxidization/hydrolysis (Mg first, then Al). At the same time, the anodic Cu fractions remain in reduced form and begin to deagglomerate as they migrate toward the solution-air interface where hydration of Cu atoms occurs followed by oxidation of the Cu, which then precipitates black cupric oxide upon drying (dehydration) ...

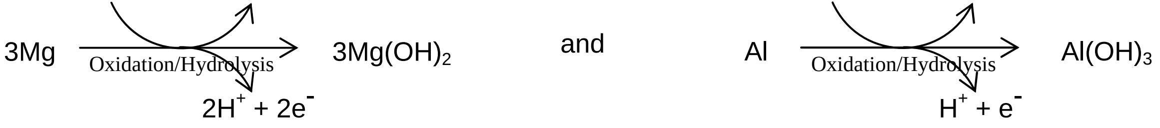

(9)

and

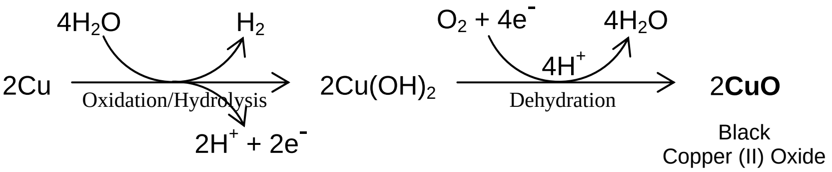

(10)

In this situation, the intermetallic phase acts as the anode (producing electrons) while the Al matrix in close proximity to the activity becomes the cathode. Hydrogen gas is evolved throughout the process. Graphical representation of the proposed scenario, using Reactions (9) and (10), is illustrated in Figure 5.

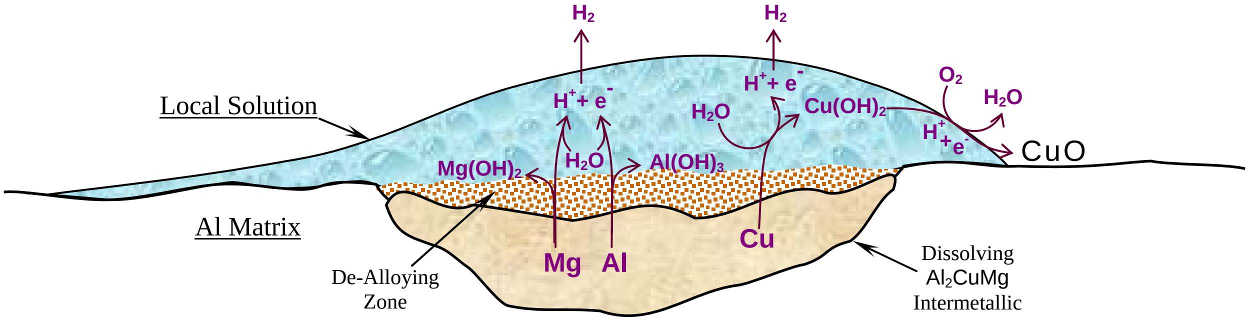

Figure 5. Galvanic couple between Mg/Al-rich intermetallic and Al matrix with the production of black copper (II) oxide.

The ‘local solution’ has been exaggerated here for illustrative purposes. In the actual field samples, moisture probably resides in and around pits and intergranular segments. Possible oxygen sources to the corrosion interface would include dissolved O_2 (from the local solution), O_2 which diffuses through the paint/coating from the outside, or O_2 which becomes available directly from the coating itself (extracted/liberated from polymer side groups and/or pigment interfaces). Sideline to Reaction (10) is the possible deposition (plating) of metallic Cu onto the Al surface (not illustrated in Figure 5). This might give a red-brown tint to the area of deposition, and since Al is anodic to Cu, these plated Cu particles/clusters would provide additional nucleation sites for more pitting corrosion.

Now the contention here is that pitting corrosion, being induced (or influenced) by local *cathodic* intermetallic phases, produces aluminum hydroxide $Al(OH)_3$ and/or the oxide Al_2O_3, which agglomerate leaving white precipitates. Conversely, when *anodic* intermetallic phases are involved, the final solid (crystalline) products will be black-to-gray copper oxide and possibly red-brown copper metal on Al matrix areas along with very small amounts of the clear-to-white hydration/oxidation products of Mg, Al and Si confined in close proximity to the dissolved intermetallic, and these oxide/hydroxides can possibly be dislodged and/or carried away by external forces.

Table 8. Measured corrosion potentials for a few intermetallic compounds (Cu, measured under similar conditions, is given for reference).

Material	*Volts*
Pure Cu	-0.11
$AlCu_3$	-0.26
$AlCu_2$	-0.32
Al_2Cu_3	-0.36
AlCu	-0.49
Al + 6% Cu	-0.67
Al + 4% Cu	-0.69
Al_2Cu	-0.70
Al + 3% Cu	-0.72
Al + 2% Cu	-0.75
Al + 1% Cu	-0.80
Al_2CuMg	-0.92
Al_2CuLi	-1.50

In addition to some of the intermetallic compounds already noted, there are a multitude of stoichiometric combinations which could form wihin the body of the alloy composition indicated in Table 6. Linus Pauling characterized hundreds of compounds including many notable (and sometimes complicated) intermetallic compositions relevant to our system such as $Al_{13}Cu_4Fe_3$, $Al_{65}Cu_{20}Fe_{14}$, Al_7Mn_2, Al_4Mn, $Al_{72}Mn_{22}Si_6$, $Al_7(Mn_1Fe)_2$ and $Al_{510}Cu_{125}Mg_{365}$ (or $Al_{51}Cu_{12.5}Mg_{36.5}$). Other researchers have reported the existence of still more Al 2024 intermetallic compounds including Al_7Cu_2Fe, $Al_5Mg_8Cu_2Si_6$, Al_5FeSi, $Al_8Mg_3FeSi_6$, and the list goes on. Many of these have been shown to exhibit anodic activity toward the Al matrix and *amongst themselves*. A short list of relatively measured corrosion EMF values for some of the simpler intermetallics is given in Table 8 (data acquired from the Internet). Here, Al + 1-2% Cu might be roughly equivalent to our 2024 test samples. There should be many possible intermetallic compounds exhibiting anodic behavior toward Al as well as toward other (cathodic) intermetallic phases.

Intergranular corrosion, like pitting, is also highly localized and the electrochemistry is similar, but corrosive growth occurs along the interfacial grain boundries of the alloy, and is not limited to the regional point of breach as with pitting. It is often accompanied by exfoliation (flaking in appearance) due to separation or lifting of the surface grains from expanding or degrading corrosion products. Intergranular corrosion may penetrate somewhat into the metal body but will often travel widely across the surface similar to the way cracks in a brick wall propagate. Since the joining interface material between grains is degraded in the process, severe cases of this type of corrosion can result in structural failure of the body.

The interfaces along grain boundries are attactive sites for migrating intermetallic compounds and for localized precipitated compounds formed from possible reactions between de-alloyed metals and certain contaminants in the region. In the ladder case, depleted zones of the base metal form along the boundry and become anodes. In any case, the particles (or precipitates) involved will either be anodic or cathodic toward the matrix (or toward themselves), but the end result is the same regardless - degradation of the intergranular bonding structure.

For wrought Al alloys which have been cast with high Mg content, production of anodic Mg-rich intermetallic compounds is inevitable during the the precipitation-hardening process. Given the composition indicated in Table 6, a multitude of intermetallics could be generated which would exhibit galvanic interactions among themselves. Many of these compounds will migrate through the alloy and concentrate, in layered fashion, along intergranular surfaces. The number of possible stoichiometries for Al-Cu-Mg-Si alloys it quite extensive and has already been well covered. In addition, the number of possible cathodic-anodic intergranular boundry layer configurations is broad. As a simplified example, consider the initiation of intergranular corrosion using a couple of likely 2024 intermetallic compounds, say Al_2Cu and $Al_5Mg_8Cu_2Si_6$, where the ladder is Mg-rich and thus, is anodic to the former. A possible scenario might be formulated as follows. A given segment of the boundry region would consist of a layer of cathodic Al_2Cu particles adjacent to a layer of anodic $Al_5Mg_8Cu_2Si_6$ particles while contaminated solution wets the boundry region. The environmental and electrochemical conditions would be very similar to that given in Figure 5. Reactions identical to those given in (9) would hydrolyze the Al and Mg components and dump them into the de-alloying zone, while Si hydrolyzes into the silicate ion which can react with either Mg or Al according to...

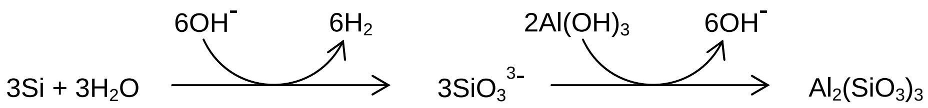

$$3Si + 3H_2O \xrightarrow{6OH^- \quad 6H_2} 3SiO_3^{3-} \xrightarrow{2Al(OH)_3 \quad 6OH^-} Al_2(SiO_3)_3$$

Here, the resulting aluminosilicate is representative of some of the possible mineral-type compounds implied earlier in Reaction (7). These kinds of compounds could also include stoichiometric fractions of Mg, Ca, H_2O and SO_4^{2-} which might be available in the local solution as calcium-magnesium-alumino silicates or sulfates.

Nevertheless, in this situation, certain layers of the boundry will oxidize/hydrolyze resulting in separation of intergranular segments and planes, as well as the production of black cupric oxide which deposits along the drying regions. An illustration of this possible scenario is dipicted in Figure 6.

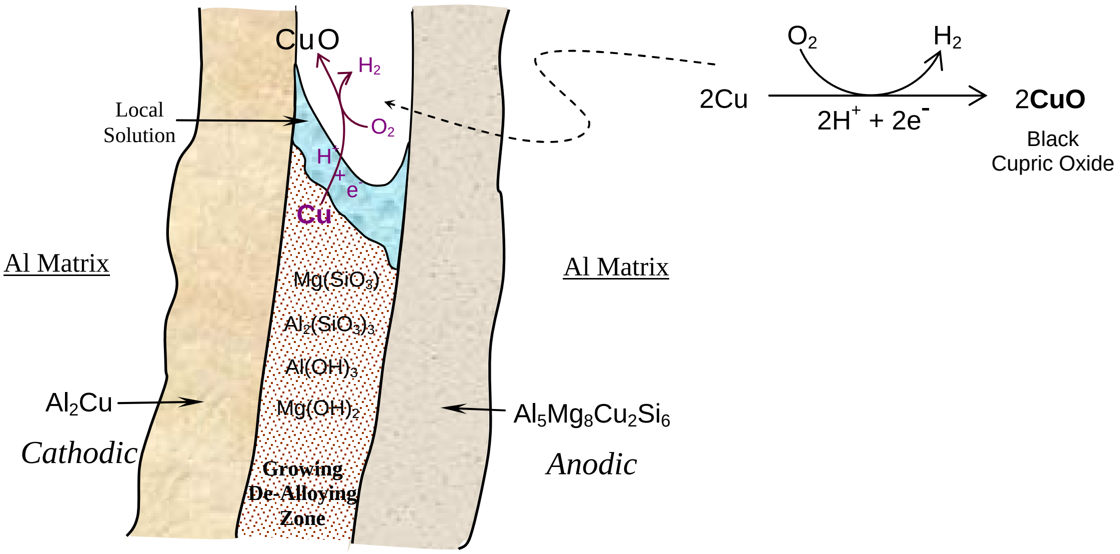

Figure 6. Illustration of possible intergranular corrosion situation that produces black copper oxide in which the boundry configuration includes interacting layers of cathodic and anodic intermetallic phases.

A final concept that needs attention here is the corrosion of copper via sulfate-reducing bacteria. There are numerous citations of corrosion events induced by these bacteria which are relevant to our study because their involvement in the corrosion process of metal products alloyed with copper is distinctly marked by localized pitting of the matrix metal and the formation of *black* sulfide metabolic products. They are ever-present in our environment, particularly in moisture-laden areas such as soils, water streams and standing water puddles. These particular micro-organisms are generally anerobic (require no oxygen), and they will typically breed on surfaces high in copper sulfate, forming black copper sulfide as well as other sulfate and sulfide rich products which can instigate pitting corrosion of less noble metals in the alloy (such as the Al matrix). Production of sulfate compounds is inevitable on copper surfaces exposed to the environment due to a 'natural sulfation' process which is fueled by atmospheric sulfur dioxide SO_2.

Formation of the corrosion-protective blue-green copper (II) sulfate patina on expose surfaces is nothing new... it has protected the Stature of Liberty for a hundred years or so, as well as many other ancient copper-based structures worldwide. However, this natural sulfation process could provide an excellent source of sulfate and sulfide ions on Al 2024 surfaces which can then etch the alumina layer in accordance with Reactions (5) and (6). Nevertheless, sulfate-reducing bacteria (SRB) will tend to form on surfaces and regions depleted in oxygen content, such as stacked or rolled 2024 aluminum panels or sheets being stored in warm, moist environments. Since the defect areas in the test samples examined for this study are black in appearance and an excess amount of sulfate was detected in the EDX compositions of our test sample areas, the probability of this mechanism as a contributing factor to the corrosion problem is significant. For corrosion growth to flourish, the alloy surface would need to contain ample Cu-rich areas to sustain bacterial growth, which is indeed the case with Al 2024 alloy systems.

While anhydrous copper sulfate is clear, the more common blue-green hydrated forms are predominant on sulfated surfaces exposed to the atmosphere. Again, natural sulfation and the formation of copper sulfate is overwhelmingly accelerated by the presence of SO_2 in rain water. Metabolic processes in the bacteria will convert the copper sulfate to black copper sulfide via anerobic reduction. The reaction scheme might be represented as...

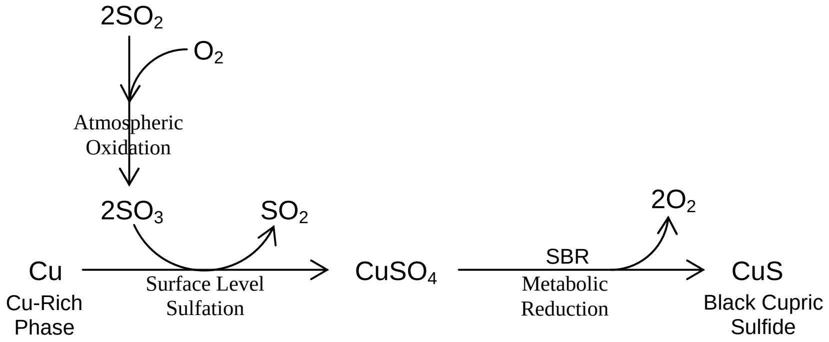

or simply...

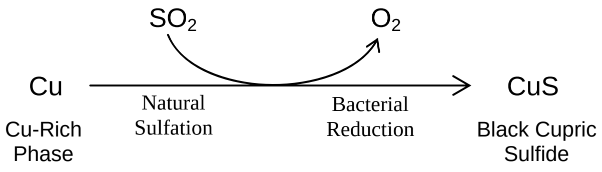

The effect of these organisms on Cu-rich surfaces coupled with moist, contaminated surroundings provides the means and the opportunity for corrosion of the less noble matrix metal to initiate. Migration of the bacteria into the intergranular regions of the material could pose a very plausible mechanism for the observed defects. There are several other bacterial strains (both aerobic and anerobic) capable of inducing corrosion processes on metal alloy surfaces but none of these will be covered here. Suffice it to say that various microbial species are known to be responsible or corrosive degradation of Al alloys.

In Closing

Both pitting and/or intergranular corrosion are believed to be likely mechanisms for the apparent degradation observed on the field return samples and some of the production detail parts noted (skins and grip plates). The Mg level appears to be abnormally high in the material examined for this study, and since de-alloyed regions of Mg can form intermetallic compounds that contain Cu *and* behave anodically toward Al, Mg could well be a major player in the corrosion processes taking place here. These conditions could possibly account for the black abberations identified as corrosion in the defect samples. Furthermore, it is believed that galvanic-type interactions play a predominant role in the corrosion processes examined here, particularly those interactions of anodic Cu-bearing intermetallic particles, granules and phases with cathodic intermetallics, as well as intermetallic interactions involving the Al matrix.

One might ask, "Why are these intermetallic entities present in our aluminum?". An adequate description of the various Al alloys is beyond the scope of this report. However, a few notes can be made regarding the 2XXX and the 5XXX series. The various Al alloy families, 1XXX through 9XXX, are typically characterized by the other metals they are mixed with during the alloying process as well as the specific regime of post-treatment processes they undergo. The primary alloying element in the 2XXX series is Cu (which can run up to ~ 5% *by weight*), while that in the 5XXX series is Mg (up to ~ 5% by weight). Both grades also contain smaller portions of other alloyed elements. For instance, second to Cu, 2024 alloy should contain 1.2-1.8% Mg. After wrought casting, a tempering (or aging) process is applied to increase hardness and strength of the material. The tempering regime used for 2024-T3 alloy involves high temperature solution treatment, cold working and natural aging, designated by the T-3 suffix (T-4 is the same as T-3 less the cold working step). Solution treatment is often referred to as 'precipitation hardening' because various intermetallic compounds (precipitates) are formed within the matrix metal during the process. Thus, these precipitates come out of the alloy solution as 'de-alloyed' particles. This is done deliberately because the particles greatly enhance the end mechanical properties. Conversely, the 5XXX materials are non-heat treatable but are hardened primarily by cold-working. Incorporation of Mg into the alloy solution will greatly improve the effects of work hardening. Solubility of the various alloying elements and their intermetallics vary widely in solid solution and is critical as to which species remain in solution, and to what degree, during processing, cold quenching, natural and artificial aging. The presence of Mg in 2024 alloys greatly accelerates and enhances precipitation hardening, and it also increases corrosion protection. The presence of Cu increases strength but usually lowers corrosion resistance. The 2XXX alloys often receive additional corrosion-inhibiting treatments (such as anodizing and/or alodine), while many of the 5XXX alloys often provide good corrosion resistance with little post-treatment. Thus, the sizes, compositions, quantities and *location* of these intermetallic particles are suspected to be directly associated with the problem at hand.

There is at least one allotrope of aluminum which is often designated as the α-Al phase and this structure solidifies into the cubic closed-packed configuration (face centered body cubic). Atoms of alloyed solutes (Cu, Mg, Si,...) probably act as interstituals occupying the holes between Al atoms, and as these interstitual atoms migrate or diffuse through the matrix structure (especially during tempering and aging), they tend to form compounds with the elements they encounter. These intermetallic compounds are usually very hard and begin to cluster as migration continues. The Al macrostructure consists of flat grains of varying sizes and as such, is roughly a lamina consisting of planes of adjoining grains that exhibit a significant degree of macro-anisotropy along with appreciable plasticity and slipping (flowing) in the solid state. The unhardened raw form leaves much to be desired regarding its strength and workability characteristics. The primary alloying elements, and most importantly, the intermetallic particles they form, will retard flowing and slipping of the matrix metal that surrounds them. The result is a metal that is both harder and stronger than pure aluminum. Unfortunately, a significant quantity of these intermetallic precipitates will migrate to the intergranular boundry regions. Clustering and agglomeration of the intermetallics will also occur which decrease their structural benefits, and these clusters will often migrate to the exterior matrix boundry. Over-aging and/or improper hardening processes could adversely affect corrosion protection performance over the lifetime of the material. In the field, additional aging and over-working caused by continued mechanical shock and vibrations, as well as wide temperature variations and cyclic thermal shocks will cause continued precipitation and migration of de-alloyed intermetallic particles through the Al matrix. These effects will result in increased accumulation of intermetallics at the grain boundries and continued clustering ('snowballing') along the way until they finally 'bloom' on the outer surface of the aluminum body. When coupled with long and intermittent exposures to contaminated moisture conditions, the surfaces will inevitably exhibit signs of corrosion activity.

Summary Points

A number of seemingly corroded areas were uncovered upon media blast and were subjected to EDX elemental analysis by the lab. The apparent compositions of these test areas were evaluated for this paper regarding their possible association with alleged field corrosion problems on several 212 M/R Blade surfaces. The chemistry of some likely reactions and associated products inferred from the EDX analysis are covered.

A mechanism is proposed to account for breaching of the oxide layer in a contaminated, moist environment containing natural ions and contaminants. Industry-standard corrosion tests may not always be ideal for characterizing particular degradation processes. Other testing regimes might be considered, such as the more aggresive HAST test.

Alumunum corrosion is believed to be highly influenced by the sizes, compositions, quantities and *location* of intermetallic precipitates, particles, agglomerates and clusters, which can eventually result in corrosive effects down field due to over-aging and prolonged exposure to moist, contaminated environments.

Pitting and intergranular corrosion are believed to be the primary failure mechanisms exhibited in these test samples and observed production details. Pitting and intergranular degradation are different manifestations from the same contributing factors involving the adverse effects of intermetallic clusters coupled with unfavorable environments.

Due to seemingly high levels of Mg in our composition, one cannot ignore the possibility that Mg degradation may be the dominant corrosion process while aluminum corrosion is secondary. From one point of view, Al alloys containing high Mg levels should exhibit improved corrosion protection. On the other hand, excessive generation of Mg-rich intermetallic particles, also containing Cu, would account for the black aberrations common to the defect areas.

Intermetallics that are cathodic to aluminum will result in formation of white precipitates (oxides, hydroxides) while anodic intermetallics can cause the formation of black copper oxide along with smaller amounts of white precipitates. Exposed copper-rich phases undergo natural sulfation which can fuel the mechanism for etching of the oxide layer.

A more extensive and elaborate EDX study might reveal critical information about the nature and composition of these intermetallic entities and their possible association with corrosion processes. EDX/SEM methods are widely used throughout the scientific field for just these types of studies.

As peculiar as it may seem, sulfate-reducing bacteria must be seriously considered as a possible source for the observed corrosion. The is due to the fact that these bacteria are known to be associated with pitting-type corrosion on metal surfaces containing copper-rich areas accompanied by the production of black sulfide products resembling some of the defective areas under investigation.

Observation of the images and defect samples gives the impression that these dark anomalies are latent and almost seem to come from within the alloy substrate. A possible theory might be formulated as follows: The bacteria migrate into the intergranular regions. In these regions, the copper level is high, sulfate is generated, local contaminants induce localized pH changes, the oxide is breached, degradative corrosion of aluminum commences as the anerobic bacteria continue to grow, producing more black sulfide.

It should be noted that this paper does not constitute a final report on the topic but only serves as an interim update centered around analysis of some of the data that has been generated for the 212 Corrosion Investigation Team. It is intended to help the team during the resolution of corrosion problems related to our products. Basically, this paper only considers a few possible factors from the material and factory point of view and does not fully take into account the impact of field conditions or customer use factors such as maintenance and operation environmental aspects. Supposedly, this information is forthcoming and could possibly have a direct effect on any pre-conclusions implied herein. Furthermore, the information presented in this paper should be considered solely as the author's opinion and as such, there are no guaranttees regarding the accuracy of implications of the concepts discussed.

References*: Quick internet searches for confirmation, correctness and enlightenment of the concepts covered.*